Technical University of Denmark

DTU

Pulsed laser deposition from ZnS and Cu2SnS3 multicomponent targets

Ettlinger, Rebecca Bolt; Cazzaniga, Andrea Carlo; Canulescu, Stela; Pryds, Nini; Schou, Jørgen

Link back to DTU Orbit

DTU Library
Technical Information Center of Denmark

Pulsed laser deposition from ZnS and Cu$_2$SnS$_3$ multicomponent targets

Rebecca Bolt Ettlinger[1]*, Andrea Cazzaniga[1], Stela Canulescu[1], Nini Pryds[2] and Jørgen Schou[1]

[1]Department of Photonics Engineering, Technical University of Denmark, DK-4000 Roskilde

[2]Department of Energy Conversion and Storage, Technical University of Denmark, DK-4000 Roskilde

*reet@fotonik.dtu.dk, +45 4677 4587, Department of Photonics Engineering, Frederiksborgvej 399, DK-4000 Roskilde, Denmark

Abstract

Thin films of ZnS and Cu$_2$SnS$_3$ have been produced by pulsed laser deposition (PLD), the latter for the first time. The effect of fluence and deposition temperature on the structure and the transmission spectrum as well as the deposition rate has been investigated, as has the stoichiometry of the films transferred from target to substrate. Elemental analysis by energy dispersive X-ray spectroscopy indicates lower S and Sn content in Cu$_2$SnS$_3$ films produced at higher fluence, whereas this trend is not seen in ZnS. The deposition rate of the compound materials measured in atoms per pulse is considerably larger than that of the individual metals, Zn, Cu, and Sn.

1 Introduction

Pulsed laser deposition (PLD) is a film deposition technique which is well suited for stoichiometric deposition of multicomponent materials [1,2]. PLD has the advantage that the atoms/molecules arriving at the substrate during deposition have a kinetic energy which may exceed the thermal energy with several orders of magnitude [3]. It is therefore possible to grow films which otherwise would require a much higher substrate temperature, and which grow under strong non-equilibrium conditions. Even for compounds with volatile elements the thin films usually exhibit optical, electronic and structural properties similar to the bulk [4–7]. However, for some materials with volatile components such as oxygen or sulfur, a part of the volatile fraction may be lost during the transfer to the substrate or during the film growth [2,8], which, for example, for oxides may lead to "metallic" rather than oxide films [9]. Therefore, in the case of oxides, a background gas is frequently used to ensure correct stoichiometry or structure of the growing film [8].

However, the procedure of compensating the loss of a volatile element with a background gas is undesirable with sulfur-containing compounds such as chalcogenides, as the gas H_2S is toxic and therefore difficult to handle. Though some researchers have used H_2S as background gas for PLD of ZnS [10], other groups have succeeded in using PLD with no background gas or with Ar to make chalcogenide thin films without significant S deficiency or loss of crystallinity, e.g., ZnS, AsS and GeS [5–7,11].

We have previously used PLD to deposit the solar cell absorber material Cu_2ZnSnS_4 (CZTS) in vacuum with no background gas, and we have observed sulfur as well as tin losses at deposition temperatures above 350°C [12]. We here deposit ZnS and Cu_2SnS_3 at temperatures below 350°C in a similar single step process with ablation of a multicomponent target made from stoichiometric chalcogenide powders. Our measurements of CZTS films deposited on fused silica demonstrate that many phases occur [12] in contrast to films deposited on typical solar cell substrates such as Mo-coated soda lime glass.

ZnS and Cu_2SnS_3 are interesting materials, not only because they are multicomponent materials with the relatively volatile element sulfur, but also because they are secondary phases in the promising solar cell material CZTS which has a band gap of 1.45 eV [13]. The additional grain boundaries from the secondary phases may trap the charge carriers in the solar cell absorber or directly lead to non-active

"dark space" in the case of ZnS with a high band gap of more than 3.5 eV [13]. These two effects are limiting the efficiency of the CZTS cell [13,14]. In addition, the cubic phases of ZnS and Cu_2SnS_3 are particularly hard to detect using X-ray diffraction within Cu_2ZnSnS_4, as the scattering peaks of all three compounds overlap [15]. Another interesting feature is that a pure absorber of Cu_2SnS_3 can be used as a solar cell absorber, albeit with a low efficiency [16].

ZnS is widely used in optical applications. It is a stable material transparent to infrared light, and in crystalline form it displays photo-, cathode- and electroluminescence when doped, e.g., with Mn [5,11]. In its cubic (zincblende) structure it has a direct band gap at about 3.54 eV, while the slightly less stable hexagonal (wurtzite) structure has a direct band gap at about 3.67 eV [17]. ZnS has been deposited by a number of different methods including thermal evaporation [18,19], metal-organic chemical vapor deposition [20], and pulsed electron deposition [21] as well as PLD [5,11,22,23].

Cu_2SnS_3 has previously been deposited as thin films by a variety of vacuum and non-vacuum methods including sulfurization of precursors produced by electron beam evaporation [16], sputtering [24], and electrodeposition [25] as well as, e.g., post-annealing of mixed elemental powders [26] and successive ionic layer absorption and reaction (SILAR) [27]. To our knowledge, Cu_2SnS_3 has not previously been deposited by PLD. Several different crystal structures have been proposed for Cu_2SnS_3 including cubic, tetragonal, and monoclinic phases with reported optical band gaps around 1 eV and with some variation in reported values [16].

In the present work we examine the structural and optical properties as well as the stoichiometry of ZnS and Cu_2SnS_3 films deposited at different fluences and substrate temperatures. Knowledge of these phases may assist us in identifying some of the phases which may occur in films of Cu_2ZnSnS_4 deposited under similar conditions.

2 Materials and methods

2.1 Pulsed laser deposition

Pulsed laser ablation was carried out with a Nd:YAG laser operating at 355 nm with a pulse duration of 6 ns and a repetition rate of 10 Hz. The target rotated as the laser rastered across an area of approx. 0.5 cm^2 at an incident angle of 45° with a spot size of 3 mm^2 except for the measurements of the deposition rate at room temperature comparing ZnS to Zn, Cu, and Sn, for which the spot size was 1 mm^2. The

substrates used in this study were fused silica. The target-substrate distance was kept constant at 45 mm and the substrate was clamped to a heated holder; the deposition temperature was monitored with a thermocouple mounted on the heater surface at the edge of the substrate. The base pressure of the deposition chamber was usually below 10^{-6} mbar.

Multicomponent hot-sintered targets were purchased from PVD products, Inc. The ZnS target was made at $1000^{o}C$ from ZnS powder, while the target with 2Cu:Sn:3S stoichiometry was made of a mixture of Cu_2S and SnS_2 powder with 1:1 molar ratio at $750^{o}C$. It is known that the detailed structure of the target does not play a significant role for the film composition except for cases where one or more components are very volatile.

The films of ZnS were deposited at room temperature to 300 °C at a laser fluence ranging from 0.8 to1 J/cm^2 as well as at room temperature at a fluence of 1.4 J/cm^2. All the ZnS films were between 200 and 250 nm thick. The films of Cu_2SnS_3 were deposited at room temperature to 250 °C at a fluence of 0.4-0.6 J/cm^2 as well as at room temperature and at 250°C at a fluence of 1.6 J/cm^2. The Cu_2SnS_3 films deposited were on average between 400 and 600 nm thick.   .

2.2 Characterization

Dektak profilometry was used to measure the thickness of deposited films of Cu_2SnS_3 and ZnS. The thickness was converted to the number of atoms per pulse assuming a bulk density of 4.079 g/cm^2 for ZnS and 5.02 g/cm^2 for Cu_2SnS_3 [17].

The transmission of the films was measured with a Cary 50 photospectrometer and the absorption coefficient α estimated from the formula α = 1/d*ln(1/T), where d is the film thickness, and T the transmission as a fraction of 1 [28]. Here we make the simplifying assumption that all the incident light is either transmitted or absorbed, with reflection and scattering being negligible. The optical band gap was determined by extrapolating the quantity $(\alpha h \nu)^2$ to zero assuming direct optical transitions.

X-ray diffraction (XRD) was carried out using a Bruker D8 diffractometer in Bragg-Brentano configuration using Cu K_{α} and Cu K_{β} radiation. The step size was 0.02° at 1 step/s for ZnS films (0.01° steps at 0.75 step/s for the room temperature film shown in Fig. 3a) and 0.01° using 0.75 step/s for the Cu_2SnS_3 films. Peaks were identified manually after stripping the Cu $K_{\alpha 2}$ signal using the program EVA and the peak patterns were matched to the relevant JCPDS files.

Energy dispersive X-ray spectroscopy (EDX) was done with 15 keV electrons with a Bruker Quantax 70 system integrated into a Hitachi TM3000 scanning electron microscope (X-ray take-off angle 25°). The average emission depth of the detected X-rays was modeled with CASINO software version 2.48 assuming a flat sample surface [29]. SEM imaging was carried out both with the Hitachi TM3000 microscope and with a Zeiss SUPRA SEM.

3 Results and discussion

The films of ZnS were transparent, appeared lightly colored due to thin film interference, and looked smooth (Fig 1a shows a ZnS film made at 200 °C; films made at other temperatures looked very similar). The films of Cu_2SnS_3 (CTS) appeared gray and were rougher than the ZnS films as observed by scanning electron microscopy. From a rather unstructured appearance at room temperature, the Cu_2SnS_3 films changed to a granular structure at 150 °C and 250 °C, as seen in Fig 1b-d. The SEM analysis revealed the presence of droplets on the surface of the Cu_2SnS_3 films with dimensions ranging from hundreds of nanometers up to one micron (Fig 1e shows a representative cross-section of the CTS film on fused SiO_2).

3.1 Deposition rate

The deposition rate of ZnS and Cu_2SnS_3 was similar and did not change significantly with increasing deposition temperature from room temperature to 300 °C for ZnS and from room temperature to 250 °C for Cu_2SnS_3 (see Fig 2). This is consistent with the observations of Xin et al. [5], who found that the growth rate of ZnS was constant from room temperature to about 300°C.

The deposition rate measurements of Zn, Cu and Sn metals taken under similar conditions [30] is significantly lower than the deposition rate of ZnS. This is partly because the heat conduction of sintered ZnS-target is much lower than for the metals and partly because the sintered target may have a high amount of defects at the grain boundaries which absorb photons at the laser energy 3.49 eV, which is slightly below the direct band gap energy of 3.54 eV for a perfect cubic-phase ZnS crystal.

3.2 Crystal structure

Figure 3 shows X-ray diffraction patterns for films of ZnS and Cu_2SnS_3 deposited at different temperatures.

ZnS films deposited at room temperature show a broad X-ray diffraction peak at the expected position of the cubic (220)/hexagonal (110) reflection (Fig. 3a). As the deposition temperature increases, this peak disappears while reflections appear at about 28.5°, at a slightly smaller angle than the cubic (111) plane/hexagonal (002) plane, as well as at about 56°, at a slightly smaller angle than the cubic (311) plane/hexagonal (112) plane. Additionally, a small peak appears at about 26° which may originate from the hexagonal (100) peak. The relatively high signal-to-noise ratio of the ZnS XRD measurements occurs because the films are thin compared to the penetration depth of the X-rays. With increased temperature the main peak at 28.5° increases in height, which could indicate an increasing fraction of crystalline versus amorphous material.

The observed peak positions are similar to observations using pulsed electron deposition by Zanettini et al. [21]. This group investigated the same range of deposition temperatures using soda lime glass substrates and observed a similar structural modification from preferential cubic (220) growth direction at room temperature to cubic (111)-growth at higher temperature. Unlike Zanettini et al., however, we do not clearly observe a complete transition to the hexagonal phase at 300 °C. In another study using the same wavelength of the third harmonic of a pulsed Nd:YAG laser (355 nm) and a substrate temperature of 400 °C, Yano et al. [23] find preferential cubic (111) and (311) direction growth similar to our results at elevated temperature. This group also found clear hexagonal-phase peaks at this relatively high growth temperature.

The X-ray diffraction patterns of the Cu_2SnS_3 films vary significantly more with deposition temperature than those of the ZnS films, as seen in Fig. 3b. The films deposited at room temperature appear amorphous. In contrast, the XRD pattern from one of the Cu_2SnS_3 films made at a substrate temperature of 150 °C clearly indicates tetragonal Cu_2SnS_3 with preferential growth in the (112) and (220) directions (expected peaks from the (200) and (312) planes are not visible). At 250 °C the diffraction peaks consistently match a mix of cubic-phase Cu_2SnS_3 with other phases, including clear peaks belonging to Cu_4SnS_4 (orthorhombic) and SnS (orthorhombic). See Table 1 (all JCPDS references in the caption of Fig. 3).

3.3 Elemental composition

Results from energy dispersive X-ray spectroscopy (EDX) show that the expected elements are present in the films (Zn and S for ZnS; Cu, Sn and S for Cu_2SnS_3). Quantifying the amount of each element is

difficult as the 15 keV electrons penetrate the layer of interest and enter partly into the substrate, such that the X-ray signal does not derive from a uniform region (see Table 1). This geometry most likely causes overestimation of the signal of Zn in ZnS and of Cu in Cu_2SnS_3. Nonetheless, films of similar thickness may be compared.

On this basis, we can show that for the ZnS films there is less S in films deposited at room temperature than at elevated temperature, while there is no difference between the composition of films deposited at 100 °C, 200 °C, and 300 °C within +/- 1 at. % equivalent to the variation between measurements of the same film. Changing the fluence from 0.8 J/cm^2 to 1.4 J/cm^2 does not measurably alter the composition of films at room temperature.

Similarly, for the Cu_2SnS_3 films, the S-content increases as the deposition temperature is raised from room temperature to 250 °C. Moreover, an increase in fluence from 0.6 J/cm^2 to 1.6 J/cm^2 results in a decrease in S and Sn content (Table 1). The S:Sn ratio is lower than three for all fluences, indicating S loss at all fluences since the Sn L-lines and S K-lines have a similar emission profile over the sample depth as modeled by Casino. The appearance of Cu_4SnS_4 and SnS together with Cu_2SnS_3 in all films made at 250 °C may be an effect of the S loss, as these compounds are S-deficient relative to Cu_2SnS_3. It is worth noting that even at high fluence at 250 °C, where the films contain least Sn and S, SnS is detected by X-ray diffraction alongside Cu_2SnS_3 and Cu_4SnS_4. However the peaks for Cu_4SnS_4 are relatively more pronounced and the SnS peaks smaller at high fluence than low fluence, matching the lower Sn content (not shown).

3.4 Optical properties

The absorption properties of the ZnS thin films as a function of deposition temperature are shown in Fig. 4a. The optical band gap of ZnS increases with the deposition temperature in a manner very similar to that observed by Zanettini et al. [21] using pulsed electron deposition (inset in Fig. 4a). The trend of increasing optical band gap with increasing temperature was also seen for laser-deposited films at temperatures from room temperature to 660 °C by Xin et al. [5], although this group did not see an optical band gap at all for films deposited at room temperature.

As estimated from Fig. 4a, the value for the optical band gap of the film deposited at 300 °C approaches the expected value of the direct band gap of cubic ZnS, i.e, 3.54 eV. Together with the

XRD data, which show an increase in crystallite formation with deposition temperature, the increase in optical band gap with temperature may reflect a change from a material that is partly amorphous with small cubic-phase crystallites to a material with larger crystals and a mix of cubic-phase and hexagonal-phase crystals, increasing the average absorption threshold.

On close comparison to the data of Zanettini et al. [21], it is interesting to note that the highest optical band gap observed by Zanettini et al. is slightly higher than that observed here, and is closer to the direct electronic band gap of hexagonal-phase ZnS, which is 3.67 eV. This may reflect a difference between pulsed laser and pulsed electron deposition, with a clearer transition to the hexagonal phase already at 300 °C with pulsed electron deposition. This would parallel the observed difference in the X-ray diffraction patterns, where Zanettini et al. observe a change to a pattern that more closely matches the hexagonal phase at 300 °C.

The transmission spectrum of the Cu_2SnS_3 thin films deposited at different temperatures is shown in Fig. 4b. It is clear that the threshold of transmission increases with temperature and the data indicate that the optical band gap of the Cu_2SnS_3 films decreases with increasing deposition temperature from about 1.55 eV to 1.35 eV. The peak or shoulder at about 1.5 eV is possibly due to thin film interference. As the temperature increases, the value of the energy gap approaches those found in literature for cubic-phase Cu_2SnS_3 of about 1 eV. However, as noted earlier, the literature values for the optical band gap vary widely. The measured band gap of ~1.45 eV for the 150 °C film, which appears from its XRD pattern to be tetragonal-phase Cu_2SnS_3, is not far from the previously reported band gap of 1.35 eV for this phase [31]. The XRD patterns of the 250 °C films indicate that we do not have pure phase Cu_2SnS_3 at this temperature but rather a mix of phases and the optical band gap must therefore reflect a mix of the absorption of these different phases.

Conclusion

In this work we have shown that pulsed laser deposition of ZnS can result in a high deposition rate, with films most likely consisting of a mix of cubic and hexagonal phases. The film quality appears to improve with substrate temperature up to 300 °C: with increasing temperature the optical band gap approaches that of the direct band gap of cubic-phase ZnS while the X-ray diffraction pattern indicates

an increasing crystalline fraction. These results are in close agreement with results from both pulsed laser deposition and pulsed electron deposition [5,21,23].

We have successfully used pulsed laser deposition to create films of Cu_2SnS_3 in the tetragonal phase at 150 °C, though more work is needed to confirm that the films are stoichiometric. These films are covered by particulates, but this issue can, for example, be reduced by applying a shorter wavelength, e.g. 248 nm, in the PLD-process [3]. At 250 °C the X-ray diffraction patterns indicate that Cu_4SnS_4 and SnS form in addition to cubic-phase Cu_2SnS_3. Energy dispersive X-ray spectroscopy shows that S and Sn content declines in the Cu_2SnS_3 films with increasing fluence. Further studies will cast more light on the secondary phases that may be formed within the range of conditions used to deposit the solar cell absorber material Cu_2ZnSnS_4. However, a complete analysis of the temperature dependence of the phase growth is not straightforward because of the many possible phases during film growth, which also may be promoted by the high kinetic energy of the arriving particles.

Figure captions

Figure 1: SEM images of as-deposited films: **a)** ZnS deposited at 200°C at a fluence of 0.9 J/cm^2; **b)** Cu_2SnS_3 film deposited at 20°C, fluence 1.4 J/cm^2, XRD pattern: amorphous; c) Cu_2SnS_3 film deposited at 150°C, fluence 0.5 J/cm^2, XRD pattern: Cu_2SnS_3 (tetragonal); d) Cu_2SnS_3 film deposited at 250°C, fluence 0.4 J/cm^2, XRD pattern: Cu_2SnS_3 (cubic), Cu_4SnS_4 (orth), SnS (orth). e) Cross section of film shown in (d). Note different scales on images.

Figure 2: Deposition rate of ZnS and Cu_2SnS_3 ablated with a 3 mm^2 spot size onto room temperature or heated substrates of fused silica or silicon. Deposition rate error derives from variation in thickness at different locations on the films. Fluence error derives from variation in laser energy and vacuum chamber window transmission during the deposition.

Figure 3: X-ray diffraction patterns for **a)** ZnS thin films and **b)** Cu_2SnS_3 thin films. $K_{\alpha 2}$ signal has been removed. The ZnS films were made with a fluence of 0.8-1 J/cm^2 while the Cu_2SnS_3 were made with a fluence of 0.5-0.6 J/cm^2. The stars in **(b)** denote peaks of orthorhombic SnS (JCPDS 75-2115) Hexagonal ZnS: JCPDS 36-1450; cubic ZnS: JCPDS 05-0566; tetragonal Cu_2SnS_3: JCPDS 89-2877; cubic Cu_2SnS_3: JCPDS 89-4714; orthorhombic Cu_4SnS_4: JCPDS 71-0129.

Figure 4: a) Optical band gap of ZnS. For ZnS the optical band gap estimate is ~ 3.15 eV, 3.3 eV, 3.5 eV, and 3.55 eV for films deposited at 20 °C, 100 °C, 200 °C, and 300 °C. The box **inset in (a)** shows the absorption threshold measured by Zanettini et al. [21] for films made by pulsed electron deposition, reproduced by permission of the authors. **b)** Transmission spectrum of Cu_2SnS_3 for films deposited at 20 °C, 150 °C, and 250 °C.

Table 1

EDX and X-ray diffraction data for films made from the ZnS target

	Fluence (J/cm^2)	Thickness (nm)*	Mean EDX emission depth (nm)**	Zn (%)***	S (%)	X-ray pattern matches
RT	0.8	230	600	60	40	ZnS cubic (220)
100	0.8	250	600	57	43	ZnS cubic (111), hex (100)
200	0.9	200	600	56	44	"
300	1.0	250	600	57	43	"
Target, unablated			*-*	*53*	*47*	*-*

EDX and X-ray diffraction data for Cu-Sn-S films made from the Cu$_2$SnS$_3$ target

	Fluence (J/cm^2)	Thickness (nm)*	Mean EDX emission depth (nm)**	Cu (%)***	Sn (%)	S (%)	X-ray pattern matches
RT	0.6	400	250	43	19	38	Amorphous
"	1.6	400	250	52	15	33	"
150	0.5	500	250	40	18	42	Cu$_2$SnS$_3$ tetragonal
250	0.6	500	250	41	17	42	Cu$_2$SnS$_3$ cubic, Cu$_2$SnS$_4$ orth, SnS orth
"	1.6	400	250	46	16	38	"
Target, unablated			*-*	*36*	*19*	*43*	*-*

* Thickness of ZnS films averaged to nearest 10 nm; thickness of Cu$_2$SnS$_3$ films averaged nearest 100 nm (due to droplets on Cu-Sn-S film surfaces, some parts of these films are thicker).

** 50 % of the X-rays reaching the EDX detector come from this depth or less; emissions are averaged from Zn and S K-lines or, as appropriate, from Cu K-lines, Sn L-lines and S K-lines (15 keV electron excitation modeled by Casino [29]).

*** Zn and Cu K-lines are used. Cu and Zn are overestimated in films thinner than the penetration depth of the electrons. The variation in measurements made on different films made under the same circumstances and on the same film measured on different days is approx. 1-2 % absolute.

References

[1]   R.W. Eason, ed., Pulsed Laser Deposition of Thin Films, Wiley, Hoboken, NJ, 2007.

[2]   J. Schou, Physical aspects of the pulsed laser deposition technique: The stoichiometric transfer of material from target to film, Appl. Surf. Sci. 255 (2009) 5191–5198.

[3]   D.H. Lowndes, Laser ablation and desorption, in: J.C. Miller, R.F. Haglund (Eds.), Exp. Methods Phys. Sci. Vol 30, Academic Press, New York, 1998: pp. 475–571.

[4]   C. Karner, P. Maguire, M. McLaughlin, S. Laverty, W.G. Graham, T. Morrow, et al., Pulsed-laser deposition of ZnS and SrS for ACTFEL and field-emission displays, in: Second Int. Conf. Sci. Technol. Disp. Phosphors, 1996.

[5]   Z.-J. Xin, R.J. Peaty, H.N. Rutt, R.W. Eason, Epitaxial growth of high-quality ZnS films on sapphire and silicon by pulsed laser deposition, Semicond. Sci. Technol. 14 (1999) 695–698.

[6]   J. Lanèok, M. Jelí, L. Jastrabí, L. Soukup, J. Oswald, K. Jurek, et al., Laser deposition of waveguiding Ti : sapphire and chalcogenide glass AsS films, in: Superf. Y Vacio, 1999: pp. 316–319.

[7]   H. Ogura, K. Matsuishi, S. Onari, Raman scattering and photodarkening of amorphous Ge(1-X)S(X) (0<X<0.62) films, J. Non-Cryst. Solids. 270 (2000) 147–153.

[8]   S. Canulescu, T. Lippert, A. Wokaun, R. Robert, D. Logvinovich, A. Weidenkaff, et al., Preparation of epitaxial La0.6Ca0.4Mn1−xFexO3 (x=0, 0.2) thin films: Variation of the oxygen content, Prog. Solid State Chem. 35 (2007) 241–248.

[9]   B. Thestrup, J. Schou, A. Nordskov, N.B. Larsen, Electrical and optical properties of thin indium tin oxide films produced by pulsed laser ablation in oxygen or rare gas atmospheres, Appl. Surf. Sci. 142 (1999) 248–252.

[10]   H. Hiramatsu, H. Ohta, M. Hirano, H. Hosono, Heteroepitaxial growth of single-phase zinc blende ZnS films on transparent substrates by pulsed laser deposition under H_2S atmosphere, Solid State Commun. 124 (2002) 411–415.

[11]   M. McLaughlin, H.F. Sakeek, P. Maguire, W.G. Graham, J. Molloy, T. Morrow, et al., Properties of ZnS thin films prepared by 248-nm pulsed laser deposition, Appl. Phys. Lett. 63 (1993) 1865.

[12]   A. Cazzaniga, A. Crovetto, S. Canulescu, J. Schou, N. Pryds, O. Hansen, Thin films of CZTS for solar cells prepared by pulsed laser deposition, submitted to Appl. Phys. B.

[13] B. Shin, O. Gunawan, Y. Zhu, N.A. Bojarczuk, S.J. Chey, S. Guha, Thin film solar cell with 8.4 % power conversion efficiency using an earth-abundant Cu2ZnSnS4 absorber, Prog. Photovoltaics Res. Appl. 21 (2013) 72–76.

[14] S. Siebentritt, Why are kesterite solar cells not 20% efficient?, Thin Solid Films. 535 (2013) 1–4.

[15] P.J. Dale, K. Hoenes, J.J. Scragg, S. Siebentritt, A review of the challenges facing kesterite based thin film solar cells, 2009 34th IEEE Photovolt. Spec. Conf. (2009) 002080–002085.

[16] N. Aihara, H. Araki, A. Takeuchi, K. Jimbo, H. Katagiri, Fabrication of Cu_2SnS_3 thin films by sulfurization of evaporated Cu-Sn precursors for solar cells, Phys. Status Solidi. 10 (2013) 1086–1092.

[17] L.I. Berger, Properties of Semiconductors, in: W.M. Haynes (Ed.), Handb. Chem. Phys., 95th ed., Taylor and Francis Group, LLT, 2014: pp. 80–85.

[18] J.T. Cox, G. Hass, Optical Properties of Zinc Sulfide in the Vacuum Ultraviolet, J. Opt. Soc. Am. 49 (1959) 807–810.

[19] X. Wu, F. Lai, L. Lin, J. Lv, B. Zhuang, Q. Yan, et al., Optical inhomogeneity of ZnS films deposited by thermal evaporation, Appl. Surf. Sci. 254 (2008) 6455–6460.

[20] A. Abounadi, M. Di Blasio, D. Bouchara, J. Calas, M. Averous, O. Briot, et al., Reflectivity and photoluminescence measurements in ZnS epilayers grown by metal-organic chemical-vapor deposition, Phys. Rev. B. 50 (1994).

[21] S. Zanettini, F. Bissoli, L. Nasi, P. Ranzieri, E. Gilioli, Low temperature pulsed electron deposition and characterization of ZnS films for application in solar cells, Cryst. Res. Technol. 46 (2011) 881–884.

[22] J.W. McCamy, D.H. Lowndes, J.D. Budai, R. A. Zuhr, X. Zhang, Epitaxial ZnS films grown on GaAs (001) and (111) by pulsed-laser ablation, J. Appl. Phys. 73 (1993) 7818.

[23] S. Yano, R. Schroeder, H. Sakai, B. Ullrich, Absorption and photocurrent properties of thin ZnS films formed by pulsed-laser deposition on quartz, Thin Solid Films 423 (2003) 273-276.

[24] H. Zhang, M. Xie, S. Zhang, Y. Xiang, Fabrication of highly crystallized Cu_2SnS_3 thin films through sulfurization of Sn-rich metallic precursors, J. Alloys Compd. 602 (2014) 199–203.

[25] D.M. Berg, R. Djemour, L. Gütay, S. Siebentritt, P.J. Dale, X. Fontane, et al., Raman analysis of monoclinic Cu_2SnS_3 thin films, Appl. Phys. Lett. 100 (2012) 192103.

[26] T. Nomura, T. Maeda, T. Wada, Preparation of Narrow Band-Gap $Cu_2Sn(S, Se)_3$ and Fabrication of Film by Non-Vacuum Process, Jpn. J. Appl. Phys. 52 (2013) 04CR08.

[27] H. Guan, H. Shen, C. Gao, X. He, Structural and optical properties of Cu_2SnS_3 and $CuSnS_4$ thin films by successive ionic layer adsorption and reaction, J. Mater. Sci.: Mater. Electron 24 (2013) 1490–1494.

[28] M. Fox, Introduction, in: Opt. Prop. Solids, Oxford University Press, 2001: p. 3.

[29] D. Drouin, A.R. Couture, D. Joly, X. Tastet, V. Aimez, R. Gauvin, CASINO V2.42: a fast and easy-to-use modeling tool for scanning electron microscopy and microanalysis users., Scanning. 29 (2007) 92–101.

[30] A. Cazzaniga, R.B. Ettlinger, S. Canulescu, J. Schou, N. Pryds, Nanosecond laser ablation and deposition of silver, copper, zinc and tin, Appl. Phys. A. 87 (2014) 89-92.

[31] P. A. Fernandes, P.M.P. Salomé, A.F. da Cunha, A study of ternary Cu_2SnS_3 and Cu_3SnS_4 thin films prepared by sulfurizing stacked metal precursors, J. Phys. D. Appl. Phys. 43 (2010) 215403.
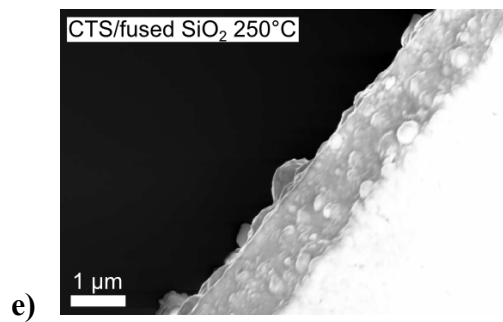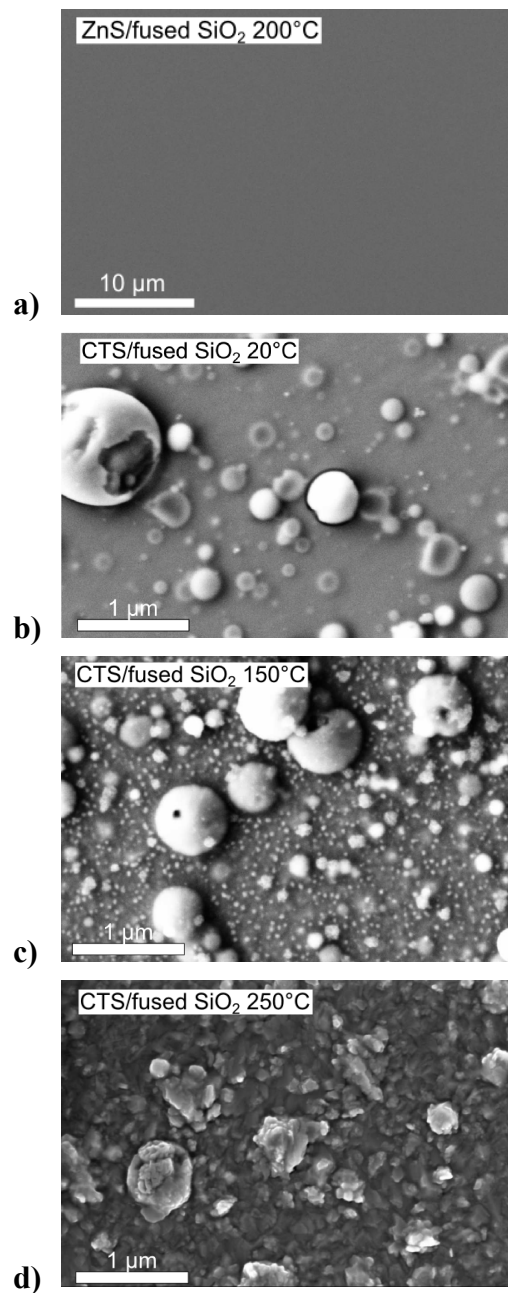
Figure 1: SEM images of as-deposited films: **a)** ZnS deposited at 200°C at a fluence of 0.9 J/cm^2; **b)** Cu$_2$SnS$_3$ film deposited at 20°C, fluence 1.4 J/cm^2, XRD pattern: amorphous; c) Cu$_2$SnS$_3$ film deposited at 150°C, fluence 0.5 J/cm^2, XRD pattern: Cu$_2$SnS$_3$ (tetragonal); d) Cu$_2$SnS$_3$ film deposited at 250°C, fluence 0.4 J/cm^2, XRD pattern: Cu$_2$SnS$_3$ (cubic), Cu$_4$SnS$_4$ (orth), SnS (orth). e) Cross section of film shown in (d). Note different scales on images.

Figure 2: Deposition rate of ZnS and Cu_2SnS_3 ablated with a 3 mm^2 spot size onto room temperature or heated substrates of fused silica or silicon. Deposition rate error in derives from variation in thickness at different locations on the films. Fluence error derives from variation in laser energy and vacuum chamber window transmission during the deposition.
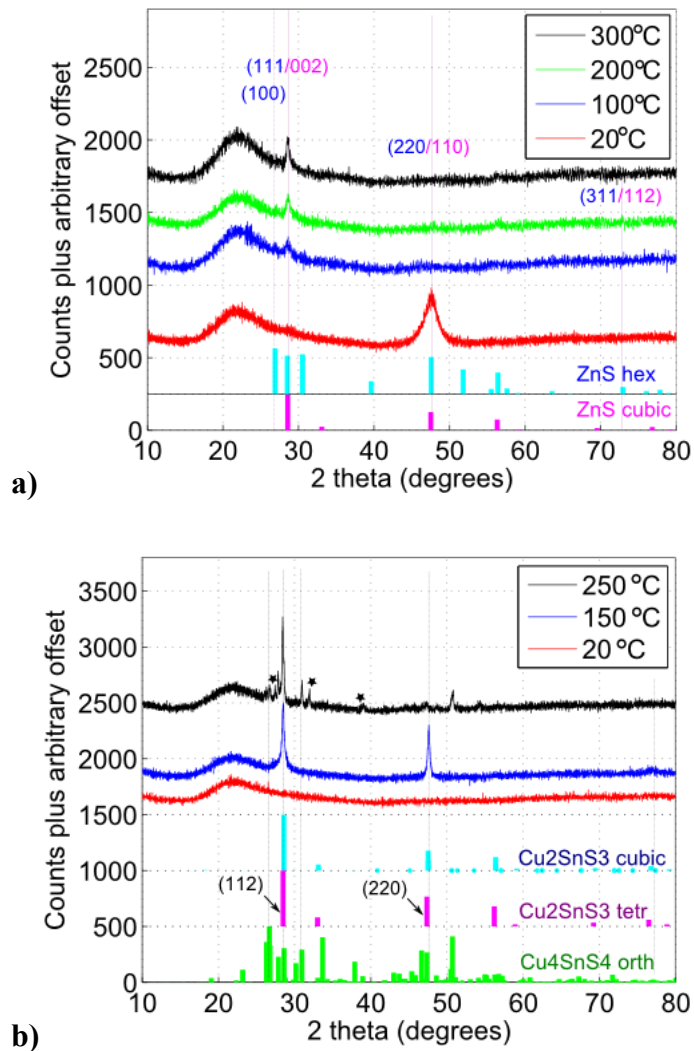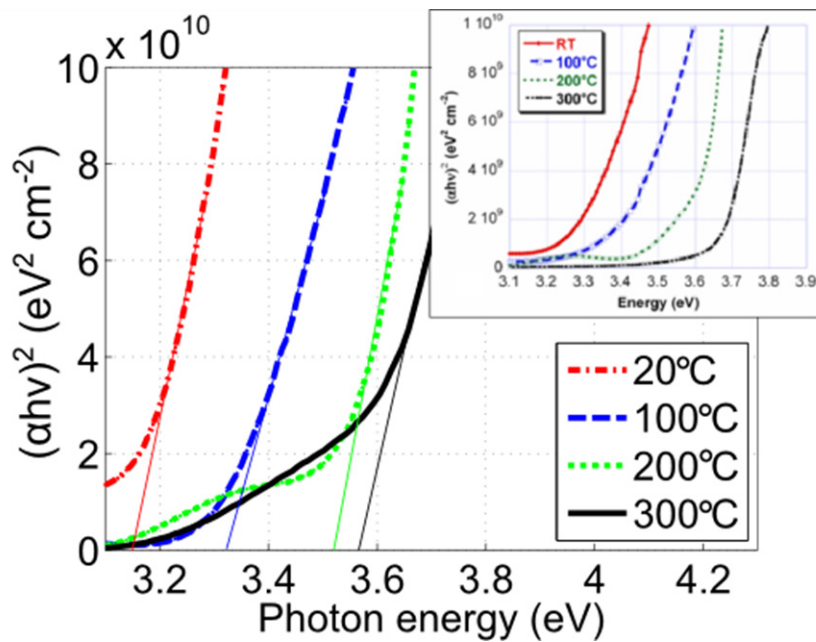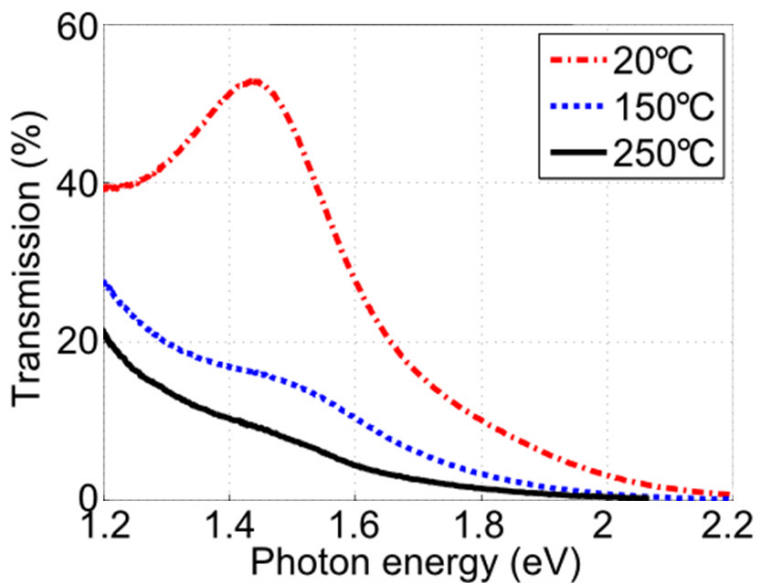
Figure 3: X-ray diffraction patterns for **a)** ZnS thin films and **b)** Cu_2SnS_3 thin films. $K_{\alpha2}$ signal has been removed. The ZnS films were made with a fluence of 0.8-1 J/cm^2 while the Cu_2SnS_3 were made with a fluence of 0.5-0.6 J/cm^2. The stars in **(b)** denote peaks of orthorhombic SnS (JCPDS 75-2115) Hexagonal ZnS: JCPDS 36-1450; cubic ZnS: JCPDS 05-0566; tetragonal Cu_2SnS_3: JCPDS 89-2877; cubic Cu_2SnS_3: JCPDS 89-4714; orthorhombic Cu_4SnS_4: JCPDS 71-0129.

a)

b)

Figure 4: a) Optical band gap of ZnS. For ZnS the optical band gap estimate is ~ 3.15 eV, 3.3 eV, 3.5 eV, and 3.55 eV for films deposited at 20 °C, 100 °C, 200 °C, and 300 °C. The box **inset in (a)** shows the absorption threshold measured by Zanettini et al. [21] for films made by pulsed electron deposition, reproduced by permission of the authors. **b)** Transmission spectrum of Cu_2SnS_3 for films deposited at 20 °C, 150 °C, and 250 °C.